PHYSICAL REVIEW D **96,** 083524 (2017)

CMB bounds on disk-accreting massive primordial black holes

Vivian Poulin,[1,2] Pasquale D. Serpico,[1,2] Francesca Calore,[1] Sébastien Clesse,[2] and Kazunori Kohri[3,4]

[1]*LAPTh, Université Savoie Mont Blanc & CNRS, 74941 Annecy Cedex, France*
[2]*Institute for Theoretical Particle Physics and Cosmology (TTK), RWTH Aachen University, D-52056 Aachen, Germany*
[3]*Theory Center, IPNS, KEK, Tsukuba 305-0801, Ibaraki, Japan*
[4]*The Graduate University of Advanced Studies (Sokendai), Tsukuba 305-0801, Ibaraki, Japan*

(Received 26 July 2017; published 24 October 2017)

Stellar-mass primordial black holes (PBH) have been recently reconsidered as a dark matter (DM) candidate after the aLIGO discovery of several binary black hole (BH) mergers with masses of tens of $M_\odot$. Matter accretion on such massive objects leads to the emission of high-energy photons, capable of altering the ionization and thermal history of the universe. This, in turn, affects the statistical properties of the cosmic microwave background (CMB) anisotropies. Previous analyses have assumed *spherical* accretion. We argue that this approximation likely breaks down and that *an accretion disk* should form in the dark ages. Using the most up-to-date tools to compute the energy deposition in the medium, we derive constraints on the fraction of DM in PBH. Provided that disks form early on, even under conservative assumptions for accretion, these constraints exclude a monochromatic distribution of PBH with masses above $\sim 2\ M_\odot$ as the dominant form of DM. The bound on the median PBH mass gets more stringent if a broad, log-normal mass function is considered. A deepened understanding of nonlinear clustering properties and BH accretion disk physics would permit an improved treatment and possibly lead to more stringent constraints.

DOI: 10.1103/PhysRevD.96.083524

I. INTRODUCTION

Despite a wealth of evidence for its existence, the nature of the dark matter (DM) composing more than 80% of the total matter content of our universe remains unknown. Particle candidates—e.g., from supersymmetric extensions of the standard model of particle physics—are still the most explored ones, in particular weakly interacting massive particles (WIMPs), in which the DM relic density $\Omega_{\rm cdm}h^2 = 0.1205$ [1] is obtained via the standard freeze-out mechanism. However, the lack of WIMP detection via collider, direct, or indirect experiments is now reviving interest in alternatives. A promising and well-studied *macroscopic* alternative to particle DM is primordial black holes (PBHs), as recently reviewed in Ref. [2]. This scenario has received a lot of attention after the aLIGO discovery of three or four binary black hole (BH) mergers of tens of solar masses [3–5], including one with a progenitor spin misaligned with the orbital momentum. Intriguingly, their merging rate is compatible with the expectation from binaries formed in present-day halos by a BH population whose density is comparable to the DM one [6,7], although Refs. [8,9] argue that this is significantly lower than the merger rate of binaries formed in the early universe, which would thus overshoot the aLIGO observed rate.

Black holes in a wide range of masses could have formed in the early universe due to the collapse of $\mathcal{O}(1)$ primordial inhomogeneities [10–12], usually associated with either extended inflationary models (such as hybrid inflation [13–16], curvaton scenarios [17,18], single-field and multi-field models in various frameworks [19–26]), or to first- and second-order phase transitions [27,28]. PBH with masses $M \lesssim 10^{-17}\ M_\odot$ evaporate into standard model particles with a blackbody spectrum (the so-called Hawking radiation [29,30]), leading to energetic particle injection which can be looked for in cosmic rays [31], γ rays [32], or CMB analysis [33]. The intermediate mass range up to stellar masses is covered by a number of lensing constraints. From low to high masses, we mention femtolensing in gamma-ray bursts [34], microlensing in high-cadence observations of M31 [35] and of the Magellanic clouds [36–38]. The latter are, however, still controversial (e.g., Ref. [39,40]), depending on the PBH clustering properties [16]; some results even point at a possible detection of anomalous microlensing events [36,37]. Additional constraints from neutron stars and white dwarfs in globular clusters also exist in this range [41,42], but they depend on astrophysical assumptions. Stellar-mass or heavier PBH are constrained by dynamical properties of ultrafaint dwarf galaxies [43–46], by halo wide binaries [47], by X-ray or radio emission [48,49], as well as by the cosmic microwave background (CMB) bounds discussed in the following.[1] Indeed, due to their gravitational attraction on the surrounding medium, such massive objects accrete matter, which heats up, gets

[1]Further constraints exist, e.g., based on the emitted gravitational wave background [50–53] or non-Gaussianities in the primordial fluctuations [54,55], which—while often quite stringent—are model dependent.

eventually ionized and emits high-energy radiation. In turn, these energetic photons can alter the ionization and thermal history of the universe, affecting the statistical properties of CMB anisotropies. Very stringent constraints (excluding PBH as DM with $M \gtrsim 0.1\ M_\odot$) have already been thus derived for this scenario a decade ago [56]. These bounds (as well as their update in Ref. [57]) have been recently revisited and corrected in Ref. [58] (see also Ref. [59]), yielding significantly weaker constraints $M \lesssim 10$–$100\ M_\odot$ if PBHs constitute the totality of the DM, depending on the assumption on radiation feedback.

Although such bounds are usually derived assuming a monochromatic PBH mass function, actual bounds on extended mass functions are typically more stringent [44,60,61]. Also, the time evolution of the initial mass function due to merging events is strongly constrained by purely gravitational CMB bounds: in each merger with comparable BH masses, a few percentage points of their mass is converted into gravitational waves, i.e., "dark" radiation, a phenomenon that cannot involve more than a small fraction of the DM, due to alterations to the Sachs-Wolfe effect. Essentially no more than one merger per PBH on average is allowed between recombination and now [62].

In this paper, we revisit the CMB anisotropy constraints on the PBH abundance, which have been derived until now assuming *spherical* accretion of matter onto BHs. We revisit this hypothesis and find plausible arguments suggesting that an *accretion disk* generically forms in the dark ages, between recombination and reionization possibly already at $z \sim \mathcal{O}(1000)$. A firm proof in that sense would require deeper studies of the nonlinear growth of structures at small scales, accounting for the peculiarities of PBH clustering and for the time-dependent building-up of the baryonic component of halos. A first step to motivate such studies, however, is to prove that they have a potentially large impact: in the presence of disks, CMB constraints on PBHs improve by (at least) two orders of magnitude, excluding the possibility that PBHs with masses $M \gtrsim 2\ M_\odot$ account for the totality of the DM. As we will argue, we expect the bounds to be greatly improved if the baryon velocity at small scales is not coherent and comparable with (or smaller than) their cosmological thermal velocity, and/or if a sizable baryon filling of the PBH halos is present already at $z \gtrsim \mathcal{O}(100)$.

This article is structured as follows: In Sec. II A, we provide a short—and necessarily incomplete—review of the current understanding of accretion and discuss its applicability in the cosmological context. The crucial arguments on why we think it is plausible that the accretion (at least the one relevant for CMB bounds) should proceed via disks is discussed in Sec. II B. In Sec. II C we review the expected high-energy luminosity associated with these accretion phenomena and describe benchmark prescriptions used afterwards. Section III describes our procedure for obtaining CMB bounds. In Sec. IV we summarize our results and draw our conclusions.

II. ACCRETION IN COSMOLOGY

A. Essentials on accretion

The problem of accretion of a point mass M moving at a constant speed $v_{\rm rel}$ in a homogeneous gas of number density n_∞ (and mass density ρ_∞, where the subscript ∞ means far away from the point mass) was first studied by Hoyle and Lyttleton [63–65] in a purely ballistic limit, i.e., accounting only for gravitational effects and no hydrodynamical or thermodynamical considerations. They found the accretion rate (natural units $c = \hbar = k_{\rm B} = 1$ are used throughout, unless stated otherwise)

$$\dot{M}_{\rm HL} \equiv \pi r_{\rm HL}^2 \rho_\infty v_{\rm rel} \equiv 4\pi\rho_\infty \frac{(GM)^2}{v_{\rm rel}^3}, \tag{1}$$

where we introduced the Hoyle-Lyttleton radius $r_{\rm HL}$, the radius of the *cylinder* effectively sweeping the medium. This model does not describe the motion of the particles once they reach the (infinitely thin and dense) accretion line in the wake of the point mass, when pressure and dissipation effects prevail. Also, it is clearly meaningless in the limit of very small velocity $v_{\rm rel}$. A first attempt to address the former problem and account for the accretion column was done by Bondi and Hoyle [66], suggesting a reduced accretion by up to a factor of 2. The second problem is linked to neglecting pressure. It has only been solved exactly for an accreting body at rest in a homogeneous gas, when the accretion is spherical by symmetry. Its rate has been computed by Bondi [67], yielding the so-called "Bondi accretion rate,"

$$\dot{M}_{\rm B} \equiv 4\pi\lambda\rho_\infty c_{\rm s,\infty} r_{\rm B}^2 \equiv 4\pi\lambda\rho_\infty \frac{(GM)^2}{c_{\rm s,\infty}^3}, \tag{2}$$

where $r_{\rm B}$ is the Bondi radius, i.e., the radius of the equivalent accreting *sphere* (as opposed to a cylinder, hence the 4π geometric factor), $c_{s,\infty}$ is the sound speed far away from the point mass, depending on the pressure P_∞ and density ρ_∞, and λ is a parameter that describes the deviation of the accretion from the Bondi idealized regime. In the cosmological plasma, one typically has:

$$c_{\rm s,\infty} = \sqrt{\frac{\gamma \mathrm{P}_\infty}{\rho_\infty}} = \sqrt{\frac{\gamma(1+x_{\rm e})T}{m_{\rm p}}} \simeq 6\,\frac{\rm km}{\rm s}\sqrt{\frac{1+z}{1000}}, \tag{3}$$

$$\Rightarrow r_{\rm B} \equiv \frac{GM}{c_{\rm s,\infty}^2} \simeq 1.2\times 10^{-4}\ {\rm pc}\,\frac{M}{M_\odot}\frac{10^3}{1+z}, \tag{4}$$

$m_{\rm p}$ being the proton mass, and γ is the polytropic equation of state coefficient for monoatomic ideal gas. The approximation at the RHS of Eq. (3) typically holds for $100 \lesssim z \lesssim 1000$. The mean cosmic gas density in the early universe is given by

$$n_\infty \simeq \frac{\rho_\infty}{m_\mathrm{p}} \simeq 200\ \mathrm{cm}^{-3}\left(\frac{1+z}{1000}\right)^3. \tag{5}$$

Finally, λ is a numerical parameter which quantifies non-gravitational forces (pressure, viscosity, radiation feedback, etc.) partially counteracting the gravitational attraction of the object. Historically, Bondi computed the maximal value of λ as a function of the equation of state of the gas, finding $\lambda \sim \mathcal{O}(1)$, ranging from 0.25 ($\gamma = 5/3$, adiabatic case) to 1.12 ($\gamma = 1$, isothermal case).

There is no exact computation of the accretion rate accounting for the finite sound speed and a displacement of the accreting object. However, as argued by Bondi in Ref. [67], a reasonable proxy can be obtained through the quadratic sum of the relative velocity and the sound speed at infinity, which leads to an effective velocity $v_\mathrm{eff}^2 = c_{s,\infty}^2 + v_\mathrm{rel}^2$. We thus define the Hoyle-Bondi radius and rate[2]

$$\dot{M}_\mathrm{HB} \equiv 4\pi\lambda\rho_\infty v_\mathrm{eff} r_\mathrm{HB}^2 \equiv 4\pi\lambda\rho_\infty \frac{(GM)^2}{v_\mathrm{eff}^3}. \tag{6}$$

Despite the fact that the Bondi analysis was originally limited to spherical accretion, this formalism is commonly used to treat nonspherical cases, with, e.g., formation of an accretion disk, by choosing an appropriate value for λ. Although it has been shown, for instance, that the simple analytical formulas can overestimate accretion in the presence of vorticity [69] or underestimate it in the presence of turbulence [70], typically Eq. (6) provides a reasonable order-of-magnitude description of the simulations (see, for instance, [71] for a recent simulation and interpolation formulas).

B. Relative baryon-PBH velocity and disk accretion in the early universe

In cosmological context, one might naively estimate the relative velocity between DM and baryons to be of the order of the thermal baryon velocity or of the speed of sound, Eq. (3). In that case, the appropriate accretion rate would be the Bondi one, Eq. (2). The situation is, however, more complicated, since at the time of recombination the sound velocity drops abruptly and the baryons, which were initially tightly coupled to the photons in a standing acoustic wave, acquire what is an eventually supersonic relative stream with respect to DM, coherent over tens of Mpc scales. In linear theory, one finds that the square root of the variance of the relative baryon-DM velocity is basically constant before recombination and then drops linearly with z as follows [72,73]:

$$\sqrt{\langle v_\mathrm{L}^2\rangle} \simeq \min\left[1, \frac{1+z}{1000}\right] \times 30\ \mathrm{km/s}. \tag{7}$$

Yet this is a linear theory result, and it is unclear if it can shed any light on the accretion, which depends on very small, sub-pc scales [Bondi radius, see Eq. (4)]. In Ref. [72], the authors first studied the problem of small-scale perturbation growth into such a configuration through a perturbative expansion of the fluid equations for DM, baryons, and the Poisson equation around the exact solution with uniform bulk motion given by Eq. (7), further assuming zero density contrast and zero Poisson potential. Their results suggest that small-scale structure formation and the baryon settling into DM potential wells is significantly delayed with respect to simple expectations. Equation (7) has also entered recent treatments of the Hoyle-Bondi PBH accretion rate, see Ref. [58], yielding a correspondingly suppressed accretion. In particular, by taking the appropriate moment of the function of velocity entering the luminosity of accreting BH over the velocity distribution, Ref. [58] found

$$v_\mathrm{eff} \equiv \left\langle \frac{1}{(c_{s,\infty}^2 + v_\mathrm{L}^2)^3} \right\rangle^{-1/6} \simeq \sqrt{c_{s,\infty}\sqrt{\langle v_\mathrm{L}^2\rangle}}, \tag{8}$$

with the last approximation only valid if $c_{s,\infty} \ll \sqrt{\langle v_\mathrm{L}^2\rangle}$, which is acceptable at early epochs after recombination, of major interest in the following.

The application of the above perturbative (but nonlinear) theory to the relative motion between PBHs and the baryon fluid down to sub-pc scales appears problematic. A first consideration is that the behavior of an ensemble of PBHs of stellar masses is very different from the "fluidlike" behavior adopted for microscopic DM candidates like WIMPs. The discreteness of PBHs is associated with a "Poissonian noise," enhancing the DM power spectrum on a small scale, down to the horizon formation one [74–77]. Our own computation suggests that a density contrast of $\mathcal{O}(1)$ is attained at $z \simeq 1000$ on a comoving scale as large as $k_\mathrm{NL} \sim 10^3\ \mathrm{Mpc}^{-1}$ for a population of $1\ M_\odot$ PBH whose number density is comparable to the DM one. Even allowing for fudge factors (e.g., $f_\mathrm{PBH} \sim 0.1$, different mass) the nonlinearity scale is unavoidably pertinent to the scales of interest. In fact, the PBH formation mechanism itself *is* a nonlinear phenomenon, and peaks theory suggests that PBHs are likely *already born* in clusters, on the verge of forming bound systems [75,78]. Our first conclusion is that the application of the scenario considered in Refs. [72,73] to the PBH case is not at all straightforward. In particular, a more meaningful background solution around which to perturb would be the one of vanishing initial baryon

[2]Actually, our rate definition is a factor of 2 larger than the original proposal, but has been confirmed as more appropriate even with numerical simulations, see Ref. [68].

perturbations in the presence of an already formed halo (and corresponding gravitational potential) on a scale $k_{\rm NL} \gtrsim 10^3$ Mpc^{-1}. A second caveat is that the treatment in Refs. [72,73] uses a fluid approximation, i.e., it does not account for "kinetic" effects such as the random (thermal) velocity distribution around the bulk motion velocity given by Eq. (7). One expects that "cold" baryons (statistically colder than the average) would already settle in the existing PBH halo at early time, forming a virialized system—albeit still underdense in baryons, with respect to the cosmological baryon-to-DM ratio. One may also worry about other effects, such as shocks and instabilities, which may hamper the applicability of the approach of Ref. [72] for too small scales and too long times.

Assuming that the overall picture remains nevertheless correct in a more realistic treatment, we expect that PBHs can generically accrete from two components: the high-velocity, free-streaming fraction at cosmological density and diminished rate of Eqs. (6) and (8), as considered in Ref. [58], and a virialized component, of initial negligible density but growing with time and eventually dominating, with typical relative velocity of the order of the virial ones. If we normalize to the Milky Way halo ($10^{12}\ M_\odot$) value $v_{\rm vir} \sim 10^{-3} c$, and adopt the simple scaling of the velocity with the halo mass over size, $v_{\rm vir}(M_{\rm halo}) \propto (M_{\rm halo}/d_{\rm halo})^{1/2} \propto M_{\rm halo}^{1/3}$, we estimate $v_{\rm vir} \sim 0.3$ km/s to 3 km/s for a halo mass of $10^3\ M_\odot$ to $10^6\ M_\odot$. The latter roughly corresponds to the smallest dwarf galaxies one is aware of; see, e.g., [79][3] At $z \simeq \mathcal{O}(1000)$ it is likely that the fast, unbound baryons constitute the dominating source of accretion. But at latest when the density of the virialized baryon component attains values comparable to the *cosmological average* density—which, given the z dependences Eqs. (3) and (7), appears unavoidable for $z \lesssim \mathcal{O}(100)$—the accretion is dominated by this halo-bound component.

After these preliminary considerations, we are ready to discuss disk formation. The basic criterion used to assess if a disk forms is to estimate the angular momentum of the material at the accretion distance: if this is sufficient to keep the matter in Keplerian rotation at a distance $r_{\rm D} \gg 3 r_{\rm S}$ (i.e.. well beyond the innermost stable orbit, where we introduced the Schwarzschild radius $r_{\rm S} \equiv 2GM$) at least for BH luminosity purposes, dominated by the region close to the BH, a disk will form [80–83]. To build up angular momentum, the material accreted at the Hoyle-Bondi distance along different directions must have appreciable velocity or density differences. The angular momentum per unit mass of the accreted gas scales like

$$l \simeq \left(\frac{\delta\rho}{\rho} + \frac{\delta v}{v_{\rm eff}}\right) v_{\rm eff}\, r_{\rm HB}, \tag{9}$$

where $\delta\rho/\rho$ represent typical inhomogeneities on the scale $r_{\rm HB}$ in the direction *orthogonal* to the relative motion of PBH-baryons, and $\delta v/v_{\rm eff}$ the analogous typical velocity gradient at the same scale (see, e.g., [83]). The above quantity can be compared to the specific angular momentum of a Keplerian orbit,

$$l_{\rm D} \simeq r_{\rm D} v_{\rm Kep}(r_{\rm D}) \simeq \sqrt{GM r_{\rm D}}, \tag{10}$$

to extract r_D. For instance, in the case of inhomogeneities, if we adopt the effective velocity on the rhs of Eq. (8) as a benchmark, as in Ref. [58], we obtain

$$\frac{r_D}{r_S} \simeq \left(\frac{\delta\rho}{\rho}\right)^2 \frac{c^2}{2v_{\rm eff}^2} \simeq 2.5 \times 10^8 \left(\frac{\delta\rho}{\rho}\right)^2 \left(\frac{1000}{1+z}\right)^{3/2}, \tag{11}$$

so that, already soon after recombination, gradients $\delta\rho/\rho \gg 10^{-4}$ in the baryon flow on the scale of the Bondi radius are sufficient for a disk to form. We find this to be largely satisfied already at $z \sim 1000$ because of the "granular" potential due to neighboring PBHs.

Equivalently, given the similar way the fractional fluctuation of velocity and density enter Eq. (9), the condition for a disk to form can be written as a lower limit on the absolute value of the velocity perturbation amounting to

$$\delta v \gg 1.5 \left(\frac{1+z}{1000}\right)^{3/2}\ \text{m/s}. \tag{12}$$

At least the component of virialized baryons, whose velocity dispersion is $\gtrsim 0.1$ km/s as argued above, should easily match this criterion.

But even for a "ideal" free-streaming homogeneous gas moving at a bulk motion comparable to Eq. (7) without any velocity dispersion, the disk formation criterion is likely satisfied if the nonlinear PBH motions at small scales are taken into account. Since this is, in general, a complicated problem, we cannot provide a cogent proof, but the following argument makes us confident that this is a likely circumstance. In general, the BH motion within its halo at very small scale is influenced by its nearest neighbors. The simplest scenario (see, for instance, [8]) amenable to analytical estimates is that a sizable fraction of PBHs form binary systems with their nearest partner, under the tidal effect of the next-to-nearest. According to [8], for PBHs constituting a sizable fraction of the DM, it is enough for their distance to be only slightly below the average distance at matter-radiation equality for a binary to form. Under the assumption of an isotropic PBH distribution and monochromatic PBH mass function of mass M, this distance can be estimated as

[3] The PBH distribution can hardly be dominated by heavier clumps, or the lack of predicted structures on the dwarf scales would automatically exclude them as the dominant DM component.

$$d \sim \left(\frac{3M}{4\pi\rho_{\mathrm{PBH}}}\right)^{1/3} = \frac{1}{1+z_{\mathrm{eq}}}\left(\frac{2GM}{H_0^2 f_{\mathrm{PBH}}\Omega_{\mathrm{DM}}}\right)^{1/3}, \quad (13)$$

i.e.,

$$d \sim 0.05 \text{ pc}\left(\frac{M}{f_{\mathrm{PBH}}M_\odot}\right)^{1/3}\frac{3400}{1+z_{\mathrm{eq}}}. \quad (14)$$

If bound, the two PBH (each of mass M) orbit around the common center of mass on an elliptical orbit whose major semiaxis is a with the Keplerian angular velocity

$$\omega = \sqrt{\frac{2GM}{a^3}}. \quad (15)$$

We conservatively assume $a = d/2$ for a quasicircular orbit, although for the very elongated orbits usually predicted for PBHs a value $a = d/4$ is closer to reality. Note that the orbital size of the order of Eq. (14) is typically larger than (or at most comparable to) the Bondi-Hoyle radius, so that to a good approximation the gas—assumed to have a bulk motion with respect to the PBH pair center of mass—accretes around a single PBH, which is however rotating with respect to it.

In the PBH rest-frame, Eq. (9) is simply replaced by

$$l \simeq \omega r_{\mathrm{HB}}^2, \quad (16)$$

or, equivalently, one can apply Eq. (12) with $\delta v = \omega r_{\mathrm{HB}}$.

If we adopt the effective velocity on the rhs of Eq. (8), this leads to the following disk formation condition ($z \lesssim 1000$):

$$f_{\mathrm{PBH}}^{1/2}\frac{M}{M_\odot} \gg \left(\frac{1+z}{730}\right)^3. \quad (17)$$

Whenever $M \gtrsim M_\odot$ and PBH constitute a sizable fraction of the DM, this is satisfied at the epoch of interest for CMB bounds.

In fact, it has been shown in Refs. [33,84] that most of the constraining power of CMB anisotropies on exotic energy injection *does not* come from redshift 1000 and above, but rather around a typical redshift of ~300 for an energy injection rate scaling like $\propto (1+z)^3$. In the problem at hand, the constraining power should be further skewed towards lower redshifts, given the growth of the signal at smaller z due to the virializing component.

We believe that these examples show that disk formation at relatively early times after recombination is a rather plausible scenario, with spherical accretion which would rather require physical justification. Note that we have improved upon the earlier discussion of this point in Ref. [56] by taking into account the essential ingredient that stellar-mass PBHs are clustered in nonlinear structures at small scales and early times, greatly differing from WIMPs in that respect. In the following, we shall assume that the disk forms at all relevant epochs for setting CMB bounds, and deduce the consequences of this ansatz. In the conclusions, we will comment on the margins for improvements over the current treatment.

C. Luminosity

In addition to $\dot{M}$, the second crucial quantity for accretion luminosity is the radiative efficiency factor ϵ, which simply relates the *accretion luminosity* L_{acc} to the accretion rate in the following way:

$$L_{\mathrm{acc}} = \epsilon \dot{M}. \quad (18)$$

The radiative efficiency is itself tightly correlated with the accretion geometry and thus the accretion rate, since it directly depends on the temperature, density, and optical thickness of the accretion region. Hence, a coherent analysis determines both parameters λ and ϵ jointly. In practice, no complete, first-principle theory exists, although a number of models have been developed to compute L_{acc} (which is the main observable in BH physics) under different assumptions and approximations. A typical fiducial value is $\epsilon = 0.1$, to be justified below. A useful benchmark upper limit to L_{acc} is the so-called Eddington luminosity, $L_E = 4\pi GMm_p/\sigma_T = 1.26\times10^{38}(M/M_\odot)\mathrm{erg/s}$, which is the luminosity at which electromagnetic radiation pressure (entering via the Thomson cross section σ_T) balances the inward gravitational force in a hydrogen gas, preventing larger accretion, unless special conditions are realized. In practice, for the parameters of cosmological interest, it turns out that we will always be below L_E.

The simplest and most complete theoretical treatment applies to spherical accretion, going back to Shapiro in Refs. [85,86] in the case of nonrotating BHs and Ref. [87] for rotating (Kerr) BHs, accounting for relativistic effects. Since we have argued that this case is unlikely to apply to the cosmological context of interest, we will not review it here, but suggest, for instance, Ref. [58] for a recent and detailed treatment. We will only refer to this case for comparison purposes, and for these cases we follow the equations in Ref. [58].

For a *moderate or low* disk accretion rate, which is the case of interest here, there are two main models:

If the radiative cooling of the gas is *efficient*, a geometrically thin disk forms, which radiates very efficiently. This is the "classical" disk solution obtained almost half a century ago by Shakura and Sunyaev [88]. In this case, the maximal energy per unit mass available is uniquely determined by the binding energy at the innermost stable orbit. This can be computed accurately in general relativity, yielding ϵ from 0.06 to 0.4 when going from a Schwarzschild to a maximally rotating Kerr BH. This range, which justifies the benchmark value $\epsilon = 0.1$ mentioned above, is often an upper limit on the radiative efficiency actually inferred from BH observations.

Also note that, since the disk can efficiently emit radiation, the temperatures characterizing the disk emission are relatively low, below a few hundreds keV.

If the radiative cooling of the gas is *inefficient*, then hot and thick/inflated disks (or torii) form, with advection and/or convective motions dominating the gas dynamics and inefficient equilibration of ion and electron temperature, with the former being much higher and able to easily reach tens of MeV. This regime is widely (albeit with some abuse of notation) known under the acronym ADAF, "advection-dominated accretion flow" (see [89] for a review). It was discovered in the pioneering article [90] and later [91], but has been extensively studied only after its "rediscovery" and 1D self-similar analytical treatment in Ref. [92]. It is worth noting that in the ADAF solution, the viscosity α plays a fundamental role in accretion: indeed, the viscously liberated energy is not radiated and dissipated away, but instead is conveyed into the optically thick gas towards the center. As a consequence, the accretion rate is typically diminished by an order of magnitude with respect to the Bondi rate with $\lambda = 1$ (see [93] for a short pedagogical overview). In practice, α is degenerate with the previously introduced parameter λ, so that one might roughly capture this effect by assuming as benchmark $\lambda = 0.1$. In "classical" ADAF models, the efficiency scales roughly linearly with $\dot{M}$, attaining (and stabilizing at) a value of the order of 0.1 only for a critical accretion which is about $0.1L_E$. Overall, this class of models provides a moderately satisfactory description (at least for $\alpha \lesssim 0.1$) of "median" X-ray observations of nuclear regions of supermassive black holes; see, e.g., [94] (in particular the lower dashed curve in Fig. 3).

A further refinement takes into account that gas outflows and jets typically accompany this regime, so that the accretion rate becomes in general a function of radius [95]. We will still normalize the (diminished) accretion rate responsible for the bulk of the luminosity to the one at the Bondi radius. For a specific example, we rely on some recent numerical solutions [96] which suggest the following: i) On the one hand, these solutions suggest that there is a more significant role of outflows, so that only ~1% of the accretion rate at the Bondi radius is ultimately accreted in the inner region most relevant for the luminosity of the disk. We shall model that by benchmarking $\lambda = 0.01$. ii) On the other hand, they suggest an increase of the fraction, δ, of the ion energy shared by electrons. Typically, in classical ADAF models, such a fraction is considered to be very small, $\delta \ll 1$. A greater efficiency δ implies a corresponding higher efficiency ϵ, somewhat intermediate between the thin disk and the classical ADAF solution, also scaling with a milder power of the mass accretion ($\epsilon \propto \dot{M}^{0.7}$) at low accretion rates. In Ref. [96], suitable fitting formulas have been provided, which we rely upon in the following. In particular, we adopt the parametrization in Eq. (11), with parameters taken from Table 1 for the ADAF accretion rate

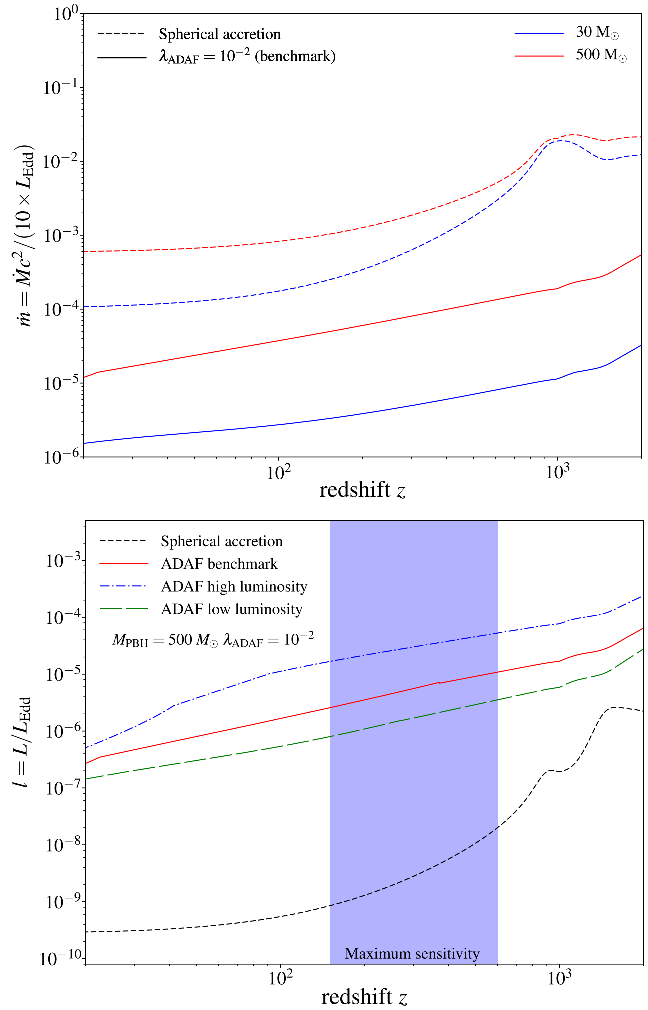

FIG. 1. *Top panel:* The dimensionless accretion rate $\dot{m}$ as a function of redshift for different accretion modeling and PBH mass. Our benchmark model corresponds to the result of simulations attested by observations. *Bottom panel:* The dimensionless luminosity l as a function of redshift for different accretion modeling. The benchmark model stands for $\delta = 0.1$, while the low-luminosity and high-luminosity scenarios correspond to $\delta = 10^{-3}$ and 0.5, respectively.

regime. In Fig. 1, we compare the spherical case with $v_{\rm eff} = \sqrt{c_{s,\infty}\langle v_L\rangle}^{1/2}$ to our benchmark $\delta = 0.1$, as well as a more optimistic $\delta = 0.5$ and a more pessimistic[4] $\delta = 10^{-3}$: the accretion rate (top panel) reduces when a disk forms (independently of δ), but the luminosity (bottom

[4]It is worth noting that such a low value is reported in Ref. [96] for historical reasons, being associated with the early analytical solutions of Ref. [92] and thus being an old benchmark, rather than because of theoretical or observational arguments related, e.g., to Sgr A^*: The authors of Ref. [96] make clear that all evidence points to a higher range for δ, with $\delta = 0.1$ being on the *conservative* side, and any $\delta \lesssim 0.3$ is in agreement with data from Sgr A^* [93].

panel) is enhanced. Since in the redshift range of interest (blue band in the bottom panel of Fig. 1, according to [33,84]) the latter is enhanced despite the fact that the former is reduced (whatever the value of δ), we expect the CMB bound to improve appreciably in our more realistic disk accretion scenario.

III. COMPUTING THE CMB BOUND

The total energy injection rate per unit volume is

$$\frac{\mathrm{d}E}{\mathrm{d}V\mathrm{d}t} = L_{\mathrm{acc}} n_{\mathrm{pbh}} = L_{\mathrm{acc}} f_{\mathrm{pbh}} \frac{\rho_{\mathrm{DM}}}{M}. \tag{19}$$

However, not all radiation is equally effective: to compute the impact on the CMB we need to quantify what amount of this injected energy is deposited into the medium, either through heating, ionization, or excitation of the atoms. The modifications of the free electron fraction x_{e} are eventually responsible for the CMB bound. For a given energy differential luminosity spectrum L_{ω}, the key information is encoded in the energy deposition functions per channel $f_c(z, x_{\mathrm{e}})$ by means of a convolution with the transfer functions $T_c(z', z, E)$ (which we take from Ref. [97]) according to

$$\begin{aligned} f_c(z, x_{\mathrm{e}}) &\equiv \frac{\mathrm{d}E/(\mathrm{d}V\mathrm{d}t)|_{\mathrm{dep},c}}{\mathrm{d}E/(\mathrm{d}V\mathrm{d}t)|_{\mathrm{inj}}} \\ &= H(z) \frac{\int \frac{\mathrm{d}\ln(1+z')}{H(z')} \int T(z', z, \omega) L_{\omega} \mathrm{d}\omega}{\int L_{\omega} \mathrm{d}\omega}. \end{aligned} \tag{20}$$

The only ingredient left is thus the spectrum of the radiation emitted via BH accretion. Note that it is only the shape that enters Eq. (20), which is indeed an efficiency function, while the overall normalization was discussed in Sec. II C. In the spherical accretion scenario (see [58,85,86]) the spectrum is dominated by Bremsstrahlung emissions, with a mildly decreasing frequency dependence over several decades and a cutoff given by the temperature of the medium near the Schwarzschild radius T_s,

$$L_{\omega} \propto \omega^{-a} \exp(-\omega/T_s), \tag{21}$$

where $T_s \sim \mathcal{O}(m_{\mathrm{e}})$ (we used 200 keV in the following for definiteness) and $|a| \lesssim 0.5$ ($a = 0$ was used in [58]).

For consistency with our discussion in Sec. II C, we base our disk accretion spectra on the numerical results for ADAF models reported in Ref. [89], Fig. 1. In particular, we adopt

$$L_{\omega} \propto \Theta(\omega - \omega_{\mathrm{min}}) \omega^{-a} \exp(-\omega/T_s), \tag{22}$$

with a choice for T_s as above. We ignore the dependence of T_s upon accretion rate and PBH mass, which is very mild in the range of concern for us. We consider $a \in [-1.3; -0.7]$, with a hardening linear in the log of $\dot{M}$ (as from the caption in that figure) with -0.7 corresponding almost to the limiting case of the thick disk. We take $\omega_{\mathrm{min}} = (10\ M_{\odot}/M)^{1/2}$ eV. Note that such a cutoff at low energy only affects the normalization at the denominator of Eq. (20), i.e., the "useful" photon fraction of the bolometric luminosity, normalized as described in Sec. II C. On the other hand, the cutoff at the numerator in Eq. (20) is, in principle, given by the ionization or excitation threshold (depending on the channel), since photons of lower energy do not contribute to the efficiency. In practice, the transfer functions are only directly available for energy injection above 5 keV. However, we can safely extrapolate the transfer function down to ~100 eV: It has been shown in Ref. [98] that the energy repartition fractions are, to an extremely good approximation, independent of the initial particle energy in the range between ~100 eV and a few keV. In fact, this behaviour is at the heart of the "low-energy code" used by authors of Ref. [97] to compute their transfer functions. Below ~100 eV, the power devoted to ionization starts to drop, and we conservatively cut the integral at the numerator at this energy. We show the $f_c(z, x_{\mathrm{e}})$ functions for the spherical accretion scenario and the disk accretion scenario in Fig. 2 (top panel) (we chose a mass which we estimate to be among the least efficient at depositing energy). We incorporated the effects of accretion into a modified version of the RECFAST module [99] of the Boltzmann solver CLASS [100]. It is enough for our purpose to work with a modified RECFAST that has been fudged to reproduce the more accurate calculations from CosmoRec [101] and HyRec [102]. The impact of the accretion on the free-electron fraction for a PBH mass of 500 $M_{\odot}$ is shown in the bottom panel of Fig. 2: it is much more pronounced in the disk accretion scenario (we chose a PBH fraction ~300 times smaller), even if the energy deposition efficiency is lower. In Fig. 3 the corresponding impact on the CMB power spectra is illustrated. The effects are typical of an electromagnetic energy injection (for a detailed review see Ref. [33]): the delayed recombination slightly shifts acoustic peaks and thus generates small wiggles at high multipoles ℓ in the residuals with respect to a standard ΛCDM scenario. Meanwhile, the increased freeze-out fraction leads to additional Thomson scattering of photons off free electrons along the line of sight, which manifests itself as a damping of temperature anisotropies and an enhanced power in the polarization spectrum. Note that, in principle, the different accretion recipes could be distinguished via a CMB anisotropy analysis. Indeed, each accretion scenario has a peculiar energy injection history which does not lead to a simple difference in the normalization: the actual shape of the power spectra slightly changes. This behavior is also present when changing the PBH mass, but is much less pronounced, albeit still above cosmic variance in the EE spectrum (not shown here to avoid cluttering). Hence, if a signal were found, it is

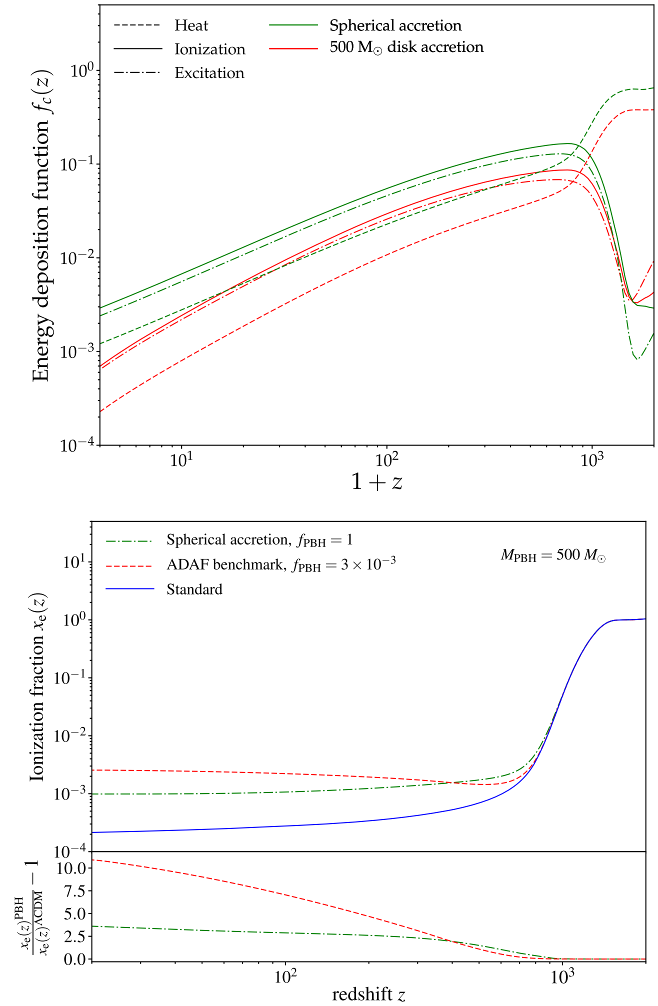

FIG. 2. *Top panel:* Energy deposition functions computed following Ref. [97] in the case of accreting PBHs. *Bottom panel:* Comparison of the free electron fractions obtained for a monochromatic population of PBHs with masses 500 $M_\odot$ depending on the accretion recipe used. The curve labeled "standard" refers to the prediction in a ΛCDM model whose parameters have been set to the best fit of Planck 2016 likelihoods high-ℓTT, TE, EE + LOWSim [1].

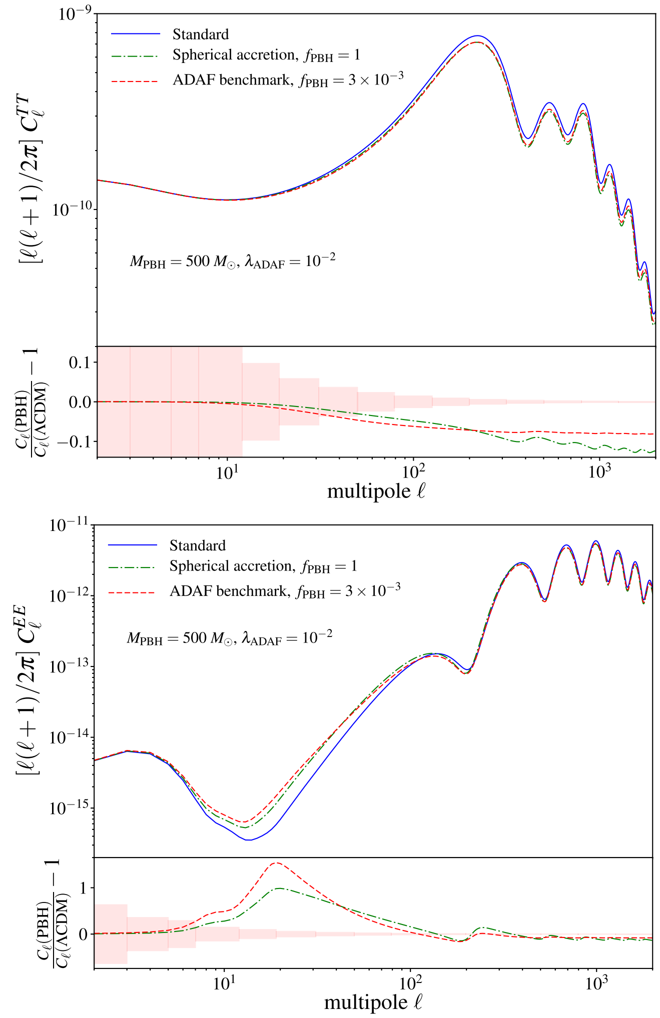

FIG. 3. CMB TT (top panel) and EE (bottom panel) power spectrum obtained for a monochromatic population of PBHs with masses 500 $M_\odot$ depending on the accretion recipe used.

conceivable that some constraints could be put on the PBH mass and (especially) accretion mechanism, but a strong statement would require better characterization of the signal, which goes beyond our present goals.

We compute the 95% C.L. bounds using data from Planck high-ℓTT, TE, EE + lensing [103] and a prior on $\tau_{\rm reio}$ [1], by running an MCMC using the MontePython package [104] associated with CLASS. For ten PBH masses log-spaced in the range $[M_{\rm min}, 1000\ M_\odot]$ we perform a fit to the data with flat priors on the following set of parameters:

$$\Lambda\mathrm{CDM} \equiv \{\omega_b, \theta_s, A_s, n_s, \tau_{\rm reio}, \omega_{\rm DM}\} + f_{\rm PBH},$$

with $M_{\rm min}$ fixed by a preliminary run where $f_{\rm PBH}$ has been set to one, and the PBH mass $M_{\rm PBH}$ has been let free to vary (with a flat prior as well).[5] We use a Choleski decomposition to handle the large number of nuisance parameters in the Planck likelihood [105]. We consider chains to have converged when the Gelman-Rubin [106] criterium gives $R-1<0.01$. First, to check our code, we run it under the *same* hypotheses as [58] (the conservative, collisional ionization case), finding the constraint $M_{\rm PBH}<150\ M_\odot$ for $f_{\rm PBH}=1$, as opposed to their $M_{\rm PBH}\lesssim 100\ M_\odot$. We attribute the 50% degradation of our bound compared with Ref. [58] to our more refined energy deposition treatment. We checked that an agreement at a similar level with Refs. [57,107] is obtained if we implement their prescriptions, but since some equations in Ref. [107] (reused in

[5]We have checked that making use of a logarithmic prior *improves* the bound by roughly 50%. We thus conservatively stick to the linear prior, which also eases comparison to previous works.

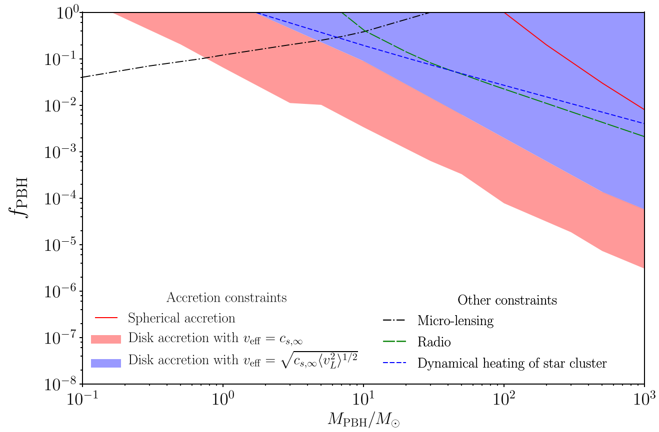

FIG. 4. Constraints on accreting PBHs as DM. Our constraints, derived from a disk accretion history [blue region: Eq. (8); light-red region: $v_{\rm eff} \simeq c_{s,\infty}$], are compared to: i) the CMB constraints obtained assuming that spherical accretion holds as in Ref. [58] (thick red line); ii) the nonobservation of microlensing events in the large Magellanic cloud as derived by the EROS-2 collaboration [38] (black dotted-dashed line); iii) the nonobservation of disk-accreting PBH at the Galactic Center in the radio band, extrapolated from Ref. [48] (green long-dashed line); iv) constraints from the disruption of the star cluster in Eridanus II [44] (blue short-dashed line, see text for details).

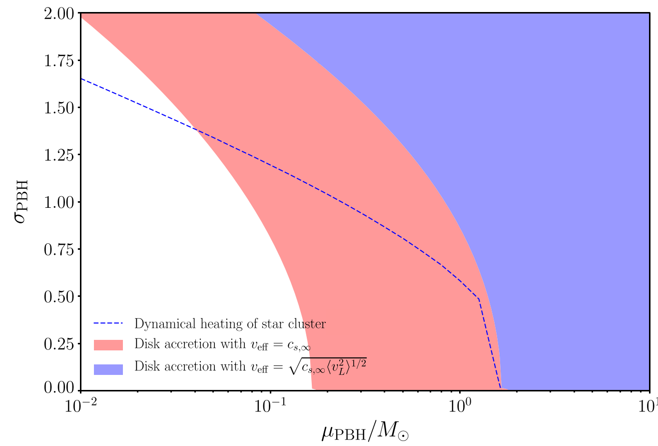

FIG. 5. Constraints on the width $\sigma_{\rm pbh}$ of a broad mass spectrum of accreting PBHs as from Eq. (25) as a function of the mean mass $\mu_{\rm PBH}$, assuming that they represent 100% of the DM. For comparison, the dashed blue line represents our calculation of the best constraint from the dynamical heating of the star cluster in the faint dwarf Eridanus II, following the method and parameters of Ref. [44].

Ref. [57]) have been shown to be erroneous [58], we do not discuss them further.

Our fiducial conservative constraints (at 95% C.L.) are represented in Fig. 4 with the blue-shaded region in the plane $(M_{\rm PBH}, f_{\rm PBH})$: We exclude PBH with masses above $\sim 2\ M_\odot$ as the dominant form of DM. The constraints can be roughly cast in the form

$$f_{\rm PBH} < \left(\frac{2\ M_\odot}{M}\right)^{1.6}\left(\frac{0.01}{\lambda}\right)^{1.6}. \tag{23}$$

This is two orders of magnitudes better than the spherical accretion scenario, and it improves significantly over the radio and X-ray constraints from Ref. [48], without dependence on the DM halo profile as in those ones. Lensing constraints are nominally better only at $M \lesssim 6\ M_\odot$. Note also the importance of the relative velocity between PBHs and accreting baryons: If instead of Eq. (8) we were to adopt $v_{\rm eff} \simeq c_{s,\infty}$, representative of a case where a density of baryons comparable to the cosmological one is captured by halos at high redshift, the bound would improve by a further order of magnitude, to $M \lesssim 0.2\ M_\odot$ (light red–shaded region in Fig. 4). This is also true, by the way, for the spherical accretion scenario, where—all other conditions being the same—adopting $v_{\rm eff} \simeq c_{s,\infty}$ would imply $M \lesssim 15\ M_\odot$, to be compared with $M \lesssim 150\ M_\odot$ previously quoted. The "known" uncertainties in disk accretion physics are probably smaller: When varying—at fixed accretion eigenvalue λ—the electrons heating parameter δ within the range described in Sec. II B, for the 30 $M_\odot$ benchmark case reported in the top panel of Fig. 1, the radiative efficiency ϵ varies by a factor of ~ 3, reflecting correspondingly on the constraints. To help readers grasp the dependence of the bound upon different parameters, we also derive a parametric bound, obtained from a run where we assumed that $v_{\rm eff}$ is constant over time (and the accretion rate is always small, i.e., $\dot{M}_{\rm B} < 10^{-3} L_{\rm Ed}$), scaling as

$$f_{\rm PBH} < \left(\frac{4\ M_\odot}{M}\right)^{1.6}\left(\frac{v_{\rm eff}}{10\ {\rm km/s}}\right)^{4.8}\left(\frac{0.01}{\lambda}\right)^{1.6}. \tag{24}$$

We have also extended the constraints to a broad log-normal mass distribution of the type

$$M\frac{{\rm d}n}{{\rm d}M} = \frac{1}{\sqrt{2\pi}\sigma M}\exp\left(\frac{-\log(M/\mu_{\rm PBH})^2}{2\sigma_{\rm pbh}^2}\right), \tag{25}$$

i.e., with mean mass $\mu_{\rm PBH}$ and width $\sigma_{\rm pbh}$. Our constraints in the plane $(\sigma_{\rm pbh}, \mu_{\rm PBH})$ assuming that PBHs represent 100% of the DM are shown in Fig. 5. It is clear that the bound on the median PBH mass is robust and can only get more stringent if a broad, log-normal mass function is considered, confirming the overall trend discussed in Ref. [61]. However, we estimate that the tightening of the constraints for a broad mass function is more modest than the corresponding one from some dynamical probes. This is illustrated by the blue dashed line in Fig. 5, which is the result of our calculation of the constraints from the disruption of the star cluster in Eridanus II, following the method and parameters of Ref. [44] (cluster mass of 3000 $M_\odot$, timescale of 12 Gyr, initial and final radius of

2 pc and 13 pc, respectively, and a cored DM density of $\rho_{\mathrm{DM}} = 1\ M_{\odot}\mathrm{pc}^{-3}$).

IV. CONCLUSIONS

The intriguing possibility that DM is made of PBHs is nowadays a subject of intense work in light of the recent gravitational wave detections of merging BHs with masses of tens of $M_{\odot}$. However, high-mass PBHs are known to accrete matter, a process that leads to the emission of a high-energy radiation able to perturb the thermal and ionization history of the universe, eventually jeopardizing the success of CMB anisotropy studies. In this computation, the geometry of the accretion, namely whether it is spherical or associated with the formation of a disk, is a major ingredient. Until now, studies have focused on the case of spherical accretion. In this work, we argued that, based on a standard criterion for disk formation, all plausible estimates suggest that a disk forms *soon after* recombination. This is essentially due to the fact that stellar-mass PBHs are in a nonlinear regime (i.e., clustered in halos of bound objects, from binaries to clumps of thousands of PBHs) at scales encompassing the Bondi radius already *before* recombination. This feature was ignored in the pioneering article [56], which assumed that massive PBHs cluster like WIMPs and deduced the adequacy of the spherical accretion approximation, eventually adopted by all subsequent studies.

Then, we have computed the effects of accretion around PBHs onto the CMB power spectra, making use of state-of-the art tools to deal with energy deposition in the primordial gas. Our 95% C.L. fiducial bounds preclude PBHs from accounting for the totality of DM if there is a monochromatic distribution of masses above $\sim 2\ M_{\odot}$. The bound on f_{PBH} improves roughly like $M^{1.6}$ with the mass. All in all, the formation of disks improves over the spherical approximation of Ref. [58] by two orders of magnitude. We also checked that the constraints derived on the monochromatic mass function apply to the average mass value of a broad, log-normal mass distribution too, actually becoming more stringent if the distribution is broader than a decade.

A realistic assessment of "known" astrophysical uncertainties, like, for instance, the electron share of the energy in ADAF models, suggests that our quantitative results can only vary within a factor of a few, not enough to qualitatively change our conclusions. Nonetheless, we believe that our constraints are conservative rather than optimistic. In particular, we assumed accretion from an environment at the *average* cosmological density: This is less and less true when PBH halos gradually capture baryonic gas in their potential wells. Alone, capturing from a pool of baryons of density comparable to the cosmological one, but bound to PBH halos, would reduce the relative PBH-baryon velocity and improve the bounds to $\sim 0.2\ M_{\odot}$. Once baryons accumulate well above the cosmological average, the accretion rate $\dot{M}$ from this bound component grows correspondingly, and the constraining power grows more than linearly with it. It would be interesting to reconsider the CMB bounds on stellar-mass PBHs once a better understanding of the halo assembly history in these scenarios is achieved, a task probably requiring dedicated hydrodynamical simulations.

Together with other constraints discussed recently (see for instance [43,44,46–49]), our bounds suggest that the possibility that PBHs of stellar masses could account for an appreciable fraction of the DM is excluded. It remains to be seen if the small f_{PBH} allowed by present constraints may still be sufficient to explain LIGO observations in terms of PBHs and, in that case, to find signatures of their primordial nature, possibly peculiar of some specific production mechanism; such signatures become all the more crucial since both PBH mass (of stellar size) and their small DM fraction (for instance, in a halo of the Milky Way size about 0.1% of the DM should be made of astrophysical BHs) cannot be easily used as diagnostic tools to discriminate PBHs from astrophysical BHs. It is worth noting that, based on the recent study [33], we expect that forthcoming CMB polarization experiments (very sensitive to energy injection) and 21 cm experiments [77,108] (the golden channel for searches looking at energy-injection during the dark ages) will be able to give more insights on PBH scenarios, including stellar-mass ones, even if the possibility that they may contribute to a high fraction of the DM has faded away.

ACKNOWLEDGMENTS

This work is partly supported by the Alexander von Humboldt Foundation (P. S.), JSPS KAKENHI Grant Nos. 26247042, JP15H05889, JP16H0877, JP17H01131 (K. K.), the Toshiko Yuasa France-Japan Particle Physics Laboratory "TYL-FJPPL" (P. S. and K. K.), as well as "Investissements d'avenir, Labex ENIGMASS" of the French ANR (V. P.). The authors warmly thank Yacine Ali-Hamoud, Juan Garcìa-Bellido, Mark Kamionkowski, Nagisa Hiroshima, and Ville Vaskonen for useful comments and discussions, and J. Lesgourgues for discussions and technical help with the CLASS implementation.

[1] N. Aghanim *et al.*, Planck intermediate results. XLVI. Reduction of large-scale systematic effects in HFI polarization maps and estimation of the reionization optical depth, Astron. Astrophys. **596**, A107 (2016).

[2] B. Carr, F. Kuhnel, and M. Sandstad, Primordial black holes as dark matter, Phys. Rev. D **94**, 083504 (2016).

[3] B. P. Abbott *et al.*, Observation of Gravitational Waves from a Binary Black Hole Merger, Phys. Rev. Lett. **116**, 061102 (2016).

[4] B. P. Abbott *et al.*, GW151226: Observation of Gravitational Waves from a 22-Solar-Mass Binary Black Hole Coalescence, Phys. Rev. Lett. **116**, 241103 (2016).

[5] B. P. Abbott *et al.*, GW170104: Observation of a 50-Solar-Mass Binary Black Hole Coalescence at Redshift 0.2, Phys. Rev. Lett. **118**, 221101 (2017).

[6] S. Bird, I. Cholis, J. B. Muoz, Y. Ali-Hamoud, M. Kamionkowski, E. D. Kovetz, A. Raccanelli, and A. G. Riess, Did LIGO Detect Dark Matter?, Phys. Rev. Lett. **116**, 201301 (2016).

[7] S. Clesse and J. Garca-Bellido, The clustering of massive primordial black holes as dark matter: Measuring their mass distribution with Advanced LIGO, Phys. Dark Universe **15**, 142 (2017).

[8] M. Sasaki, T. Suyama, T. Tanaka, and S. Yokoyama, Primordial Black Hole Scenario for the Gravitational-Wave Event GW150914, Phys. Rev. Lett. **117**, 061101 (2016).

[9] M. Raidal, V. Vaskonen, and H. Veerme, Gravitational Waves from Primordial Black Hole Mergers, J. Cosmol. Astropart. Phys. 09 (2017) 037.

[10] B. J. Carr and S. W. Hawking, Black holes in the early Universe, Mon. Not. R. Astron. Soc. **168**, 399 (1974).

[11] B. J. Carr, The Primordial black hole mass spectrum, Astrophys. J. **201**, 1 (1975).

[12] T. Harada, C.-M. Yoo, and K. Kohri, Threshold of primordial black hole formation, Phys. Rev. D **88**, 084051 (2013); Phys. Rev. D **89**, 029903(E) (2014).

[13] J. Garcia-Bellido, A. D. Linde, and D. Wands, Density perturbations and black hole formation in hybrid inflation, Phys. Rev. D **54**, 6040 (1996).

[14] D. H. Lyth, Primordial black hole formation and hybrid inflation, arXiv:1107.1681.

[15] E. Bugaev and Klimai, Formation of primordial black holes from non-Gaussian perturbations produced in a waterfall transition, Phys. Rev. D **85**, 103504 (2012).

[16] S. Clesse and J. Garcia-Bellido, Massive primordial black holes from hybrid inflation as dark matter and the seeds of galaxies, Phys. Rev. D **92**, 023524 (2015).

[17] K. Kohri, C.-M. Lin, and T. Matsuda, Primordial black holes from the inflating curvaton, Phys. Rev. D **87**, 103527 (2013).

[18] M. Kawasaki, N. Kitajima, and T. T. Yanagida, Primordial black hole formation from an axionlike curvaton model, Phys. Rev. D **87**, 063519 (2013).

[19] M. Kawasaki, A. Kusenko, Y. Tada, and T. T. Yanagida, Primordial black holes as dark matter in supergravity inflation models, Phys. Rev. D **94**, 083523 (2016).

[20] J. Garcia-Bellido, M. Peloso, and C. Unal, Gravitational waves at interferometer scales and primordial black holes in axion inflation, J. Cosmol. Astropart. Phys. 12 (2016) 031.

[21] J. Garcia-Bellido and E. Ruiz Morales, Primordial black holes from single field models of inflation, arXiv:1702.03901.

[22] V. Domcke, F. Muia, M. Pieroni, and L. T. Witkowski, PBH dark matter from axion inflation J. Cosmol. Astropart. Phys. 07 (2017) 048.

[23] C. Germani and T. Prokopec, On primordial black holes from an inflection point, arXiv:1706.04226.

[24] J. M. Ezquiaga, J. Garcia-Bellido, and E. Ruiz Morales, Primordial black hole production in critical Higgs inflation, arXiv:1705.04861.

[25] K. Kannike, L. Marzola, M. Raidal, and H. Veerme, Single field double inflation and primordial black holes, J. Cosmol. Astropart. Phys. 09 (2017) 020.

[26] H. Motohashi and W. Hu, Primordial black holes and slow-roll violation, Phys. Rev. D **96**, 063503 (2017).

[27] K. Jedamzik and J. C. Niemeyer, Primordial black hole formation during first order phase transitions, Phys. Rev. D **59**, 124014 (1999).

[28] S. G. Rubin, A. S. Sakharov, and M. Khlopov, The Formation of primary galactic nuclei during phase transitions in the early universe, J. Exp. Theor. Phys. **91**, 921 (2001); **92**, 921 (2001).

[29] S. W. Hawking, Particle Creation by Black Holes, Commun. Math. Phys. **43**, 199 (1975); Commun. Math. Phys. **43**, 167 (1975).

[30] S. W. Hawking, Black hole explosions, Nature (London) **248**, 30 (1974).

[31] A. Barrau, G. Boudoul, F. Donato, D. Maurin, P. Salati, and R. Taillet, Anti-protons from primordial black holes, Astron. Astrophys. **388**, 676 (2002).

[32] B. J. Carr, K. Kohri, Y. Sendouda, and J. Yokoyama, Constraints on primordial black holes from the Galactic gamma-ray background, Phys. Rev. D **94**, 044029 (2016).

[33] V. Poulin, J. Lesgourgues, and D. Serpico, Cosmological constraints on exotic injection of electromagnetic energy, J. Cosmol. Astropart. Phys. 03 (2017) 043.

[34] A. Barnacka, J.-F. Glicenstein, and R. Moderski, New constraints on primordial black holes abundance from femtolensing of gamma-ray bursts, Phys. Rev. D **86**, 043001 (2012).

[35] H. Niikura, M. Takada, N. Yasuda, R. H. Lupton, T. Sumi, S. More, A. More, M. Oguri, and M. Chiba, Microlensing constraints on 10^{-10} $M_\odot$-scale primordial black holes from high-cadence observation of M31 with Hyper Suprime-Cam, arXiv:1701.02151.

[36] N. Palanque-Delabrouille, Microlensing towards the small magellanic cloud. eros 2 first year survey, Astron. Astrophys. **332**, 1 (1998).

[37] C. Alcock *et al.*, The MACHO project: Microlensing results from 5.7 years of LMC observations, Astrophys. J. **542**, 281 (2000).

[38] P. Tisserand *et al.*, Limits on the Macho content of the galactic halo from the EROS-2 survey of the Magellanic clouds, Astron. Astrophys. **469**, 387 (2007).

[39] M. R. S. Hawkins, The case for primordial black holes as dark matter, Mon. Not. R. Astron. Soc. **415**, 2744 (2011).

[40] A. M. Green, Astrophysical uncertainties on stellar microlensing constraints on multi-Solar mass primordial black hole dark matter, Phys. Rev. D **96**, 043020 (2017).
[41] F. Capela, M. Pshirkov, and Tinyakov, Constraints on primordial black holes as dark matter candidates from capture by neutron stars, Phys. Rev. D **87**, 123524 (2013).
[42] F. Capela, M. Pshirkov, and Tinyakov, Constraints on primordial black holes as dark matter candidates from star formation, Phys. Rev. D **87**, 023507 (2013).
[43] T. D. Brandt, Constraints on MACHO dark matter from compact stellar systems in ultra-faint dwarf galaxies, Astrophys. J. **824**, L31 (2016).
[44] A. M. Green, Microlensing and dynamical constraints on primordial black hole dark matter with an extended mass function, Phys. Rev. D **94**, 063530 (2016).
[45] T. S. Li *et al.*, Farthest neighbor: The distant Milky Way satellite Eridanus II, Astrophys. J. **838**, 8 (2017).
[46] S.M. Koushiappas and A. Loeb, Dynamics of dwarf galaxies disfavor stellar-mass black hole dark matter, Phys. Rev. Lett. **119**, 041102 (2017).
[47] M. A. Monroy-Rodríguez and C. Allen, The end of the MACHO era, revisited: New limits on MACHO masses from halo hide binaries, Astrophys. J. **790**, 159 (2014).
[48] D. Gaggero, G. Bertone, F. Calore, R. M. T. Connors, M. Lovell, S. Markoff, and E. Storm, Searching for Primordial Black Holes in the Radio and X-ray Sky, Phys. Rev. Lett. **118**, 241101 (2017).
[49] Y. Inoue and A. Kusenko, A new X-ray bound on primordial black holes density, arXiv:1705.00791.
[50] T. Nakama, J. Silk, and M. Kamionkowski, Stochastic gravitational waves associated with the formation of primordial black holes, Phys. Rev. D **95**, 043511 (2017).
[51] S. Clesse and J. Garca-Bellido, Detecting the gravitational wave background from primordial black hole dark matter, arXiv:1610.08479.
[52] K. Schutz and A. Liu, Pulsar timing can constrain primordial black holes in the LIGO mass window, Phys. Rev. D **95**, 023002 (2017).
[53] I. Cholis, On the gravitational wave background from black hole binaries after the first LIGO detections, J. Cosmol. Astropart. Phys. 06 (2017) 037.
[54] Y. Tada and S. Yokoyama, Primordial black holes as biased tracers, Phys. Rev. D **91**, 123534 (2015).
[55] S. Young and C. T. Byrnes, Signatures of non-Gaussianity in the isocurvature modes of primordial black hole dark matter, J. Cosmol. Astropart. Phys. 04 (2015) 034.
[56] M. Ricotti, J. P. Ostriker, and K. J. Mack, Effect of primordial black holes on the cosmic microwave background and cosmological parameter estimates, Astrophys. J. **680**, 829 (2008).
[57] B. Horowitz, Revisiting primordial black hole constraints from ionization history, arXiv:1612.07264.
[58] Y. Ali-Hamoud and M. Kamionkowski, Cosmic microwave background limits on accreting primordial black holes, Phys. Rev. D **95**, 043534 (2017).
[59] D. Aloni, K. Blum, and R. Flauger, Cosmic microwave background constraints on primordial black hole dark matter, J. Cosmol. Astropart. Phys. 05 (2017) 017.
[60] F. Khnel and K. Freese, Constraints on primordial black holes with extended mass functions, Phys. Rev. D **95**, 083508 (2017).
[61] B. Carr, M. Raidal, T. Tenkanen, V. Vaskonen, and H. Veerme, Primordial black hole constraints for extended mass functions, Phys. Rev. D **96**, 023514 (2017).
[62] V. Poulin, D. Serpico, and J. Lesgourgues, A fresh look at linear cosmological constraints on a decaying dark matter component, J. Cosmol. Astropart. Phys. 08 (2016) 036.
[63] F. Hoyle and R. A. Lyttleton, The effect of interstellar matter on climatic variation, Proc. Cambridge Philos. Soc. **35**, 405 (1939).
[64] F. Hoyle and R. A. Lyttleton, On the physical aspects of accretion by stars, Proc. Cambridge Philos. Soc. **36**, 424 (1940).
[65] F. Hoyle and R. A. Lyttleton, On the accretion of interstellar matter by stars, Proc. Cambridge Philos. Soc. **36**, 325 (1940).
[66] H. Bondi and F. Hoyle, On the mechanism of accretion by stars, Mon. Not. R. Astron. Soc. **104**, 273 (1944).
[67] H. Bondi, On spherically symmetrical accretion, Mon. Not. R. Astron. Soc. **112**, 195 (1952).
[68] E. Shima, T. Matsuda, H. Takeda, and K. Sawada, Hydrodynamic calculations of axisymmetric accretion flow, Mon. Not. R. Astron. Soc. **217**, 367 (1985).
[69] M. R. Krumholz, C. F. McKee, and R. I. Klein, Bondi accretion in the presence of vorticity, Astrophys. J. **618**, 757 (2005).
[70] M. R. Krumholz, C. F. McKee, and R. I. Klein, Bondi-Hoyle accretion in a turbulent medium, Astrophys. J. **638**, 369 (2006).
[71] I. El Mellah and F. Casse, Numerical simulations of axisymmetric hydrodynamical Bondi-Hoyle accretion onto a compact object, Mon. Not. R. Astron. Soc. **454**, 2657 (2015).
[72] D. Tseliakhovich and C. Hirata, Relative velocity of dark matter and baryonic fluids and the formation of the first structures, Phys. Rev. D **82**, 083520 (2010).
[73] C. Dvorkin, K. Blum, and M. Kamionkowski, Constraining dark matter-baryon scattering with linear cosmology, Phys. Rev. D **89**, 023519 (2014).
[74] N. Afshordi, McDonald, and D. N. Spergel, Primordial black holes as dark matter: The Power spectrum and evaporation of early structures, Astrophys. J. **594**, L71 (2003).
[75] J. R. Chisholm, Clustering of primordial black holes: Basic results, Phys. Rev. D **73**, 083504 (2006).
[76] K. M. Zurek and C. J. Hogan, White noise from dark matter: 21 cm observations of early baryon collapse, Phys. Rev. D **76**, 063002 (2007).
[77] J.-O. Gong and N. Kitajima, Small-scale structure and 21 cm fluctuations by primordial black holes, J. Cosmol. Astropart. Phys. 08 (2017) 017.
[78] J. R. Chisholm, Clustering of primordial black holes. II. Evolution of bound systems, Phys. Rev. D **84**, 124031 (2011).
[79] V. Bonnivard *et al.*, Dark matter annihilation and decay in dwarf spheroidal galaxies: The classical and ultrafaint dSphs, Mon. Not. R. Astron. Soc. **453**, 849 (2015).

[80] S. L. Shapiro and A. P. Lightman, Black holes in X-ray binaries—Marginal existence and rotation reversals of accretion disks, Astrophys. J. **204**, 555 (1976).

[81] J. R. Ipser and R. H. Price, Accretion onto pregalactic black holes, Astrophys. J. **216**, 578 (1977).

[82] M. Ruffert, Non-axisymmetric wind-accretion simulations. II. Density gradients, Astron. Astrophys. **346**, 861 (1999).

[83] E. Agol and M. Kamionkowski, X-rays from isolated black holes in the Milky Way, Mon. Not. R. Astron. Soc. **334**, 553 (2002).

[84] T. R. Slatyer and C.-L. Wu, General constraints on dark matter decay from the cosmic microwave background, Phys. Rev. D **95**, 023010 (2017).

[85] S. L. Shapiro, Accretion onto black holes: The emergent radiation spectrum, Astrophys. J. **180**, 531 (1973).

[86] S. L. Shapiro, Accretion onto black holes: The emergent radiation spectrum. II. Magnetic effects, Astrophys. J. **185**, 69 (1973).

[87] S. L. Shapiro, Accretion onto black holes: The emergent radiation spectrum. III. Rotating (kerr) black holes, Astrophys. J. **189**, 343 (1974).

[88] N. I. Shakura and R. A. Sunyaev, Black holes in binary systems. Observational appearance, Astron. Astrophys. **24**, 337 (1973).

[89] F. Yuan and R. Narayan, Hot accretion flows around black holes, Annu. Rev. Astron. Astrophys. **52**, 529 (2014).

[90] S. Ichimaru, Bimodal behavior of accretion disks—Theory and application to Cygnus X-1 transitions, Astrophys. J. **214**, 840 (1977).

[91] M. J. Rees, E. S. Phinney, M. C. Begelman, and R. D. Blandford, Ion supported tori and the origin of radio jets, Nature (London) **295**, 17 (1982).

[92] R. Narayan and I.-s. Yi, Advection dominated accretion: A Selfsimilar solution, Astrophys. J. **428**, L13 (1994).

[93] R. Narayan, Why do agn lighthouses switch off?, arXiv:astro-ph/0201260.

[94] S. Pellegrini, Nuclear accretion in galaxies of the local Universe: Clues from Chandra observations, Astrophys. J. **624**, 155 (2005); **636**, 564(E) (2006).

[95] R. D. Blandford and M. C. Begelman, On the fate of gas accreting at a low rate onto a black hole, Mon. Not. R. Astron. Soc. **303**, L1 (1999).

[96] F.-G. Xie and F. Yuan, Radiative efficiency of hot accretion flows, Mon. Not. R. Astron. Soc. **427**, 1580 (2012).

[97] T. R. Slatyer, Indirect dark matter signatures in the cosmic dark ages II. Ionization, heating and photon production from arbitrary energy injections, Phys. Rev. D **93**, 023521 (2016).

[98] S. Galli, T. R. Slatyer, M. Valdes, and F. Iocco, Systematic uncertainties in constraining dark matter annihilation from the cosmic microwave background, Phys. Rev. D **88**, 063502 (2013).

[99] S. Seager, D. D. Sasselov, and D. Scott, A new calculation of the recombination epoch, Astrophys. J. **523**, L1 (1999).

[100] D. Blas, J. Lesgourgues, and T. Tram, The Cosmic Linear Anisotropy Solving System (CLASS) II: Approximation schemes, J. Cosmol. Astropart. Phys. 07 (2011) 034.

[101] J. Chluba and R. M. Thomas, Towards a complete treatment of the cosmological recombination problem, Mon. Not. R. Astron. Soc. **412**, 748 (2011).

[102] Y. Ali-Haïmoud and C. M. Hirata, HyRec: A fast and highly accurate primordial hydrogen and helium recombination code, Phys. Rev. D **83**, 043513 (2011).

[103] P. A. R. Ade *et al.*, Planck 2015 results. XIII. Cosmological parameters, Astron. Astrophys. **594**, A13 (2016).

[104] B. Audren, J. Lesgourgues, K. Benabed, and S. Prunet, Conservative constraints on early cosmology: An illustration of the Monte Python cosmological parameter inference code, J. Cosmol. Astropart. Phys. 02 (2013) 001.

[105] A. Lewis, Efficient sampling of fast and slow cosmological parameters, Phys. Rev. D **87**, 103529 (2013).

[106] A. Gelman and D. B. Rubin, Inference from iterative simulation using multiple sequences, Stat. Sci. **7**, 457 (1992).

[107] M. Ricotti, Bondi accretion in the early universe, Astrophys. J. **662**, 53 (2007).

[108] H. Tashiro and N. Sugiyama, The effect of primordial black holes on 21-cm fluctuations, Mon. Not. R. Astron. Soc. **435**, 3001 (2013).